WASP – A System and Algorithms for Accurate Radio Localization Using Low-Cost Hardware

T. Sathyan, *Member, IEEE* D. Humphrey, *Member, IEEE* and M. Hedley *Senior Member, IEEE*

Abstract—In this paper we present a low-cost wireless sensor network (WSN) platform, called Wireless Ad hoc System for Positioning (WASP), that has been developed for high accuracy localization and tracking. This platform uses the time of arrival (TOA) of beacon signals periodically transmitted by the nodes at known times for localization. The system was designed to have a unique tradeoff between hardware complexity and processing complexity to provide high accuracy at minimal cost in complex radio propagation environments. To enable the system to perform well in realistic environments it was also necessary to develop novel extensions to existing algorithms for the measurement of TOA, localization, and tracking. In this paper we describe the architecture, hardware, and algorithms of WASP and present results based on field trials conducted in different radio propagation environments. The results show that WASP achieves a ranging accuracy of 0.15 m outdoors and 0.5 m indoors when around twelve anchor nodes are used. These accuracies are achieved with operating range of up to 200 m outdoors and 30 m indoors. This compares favorably to other published results for systems operating in realistic environments.

Index Terms—Wireless sensor networks, radio localization and tracking, time of arrival, two-way ranging, multipath, indoor propagation, least squares estimation.

I. Introduction

Wireless sensor networks (WSN), consisting of small, low-cost, and self-organizing nodes that are suitable for rapid deployment promise a wide range of applications such as habitat monitoring, assisting emergency first responders, automation and safety in the mining industry, and performance monitoring of athletes. For many WSN applications localization, i.e., the determination of the spatial coordinates, of the nodes is an important requirement [24].

Existing localization technologies such as the well-known Global Positioning System (GPS) [13] can be used for some WSN applications but for many others suitable technology does not exist or is too expensive. For example, GPS generally does not work indoors or underground, and performs poorly in urban canyons. Even in clear outdoor environments the accuracy provided by low-cost GPS receivers (of the order of several of meters) is not adequate for applications such as tracking athletes for performance monitoring.

Several research groups [1], [2], [21], [25], [27] have been working to develop a high accuracy terrestrial localization systems (an extensive list of publications in this area can be found in [19]) using different technologies, although none are

The authors are with the Information and Communication Technologies Center, Commonwealth Scientific and Industrial Research Organization (CSIRO), Marfield, Australia. Postal Address: PO Box 76, Epping, NSW, 1710, Australia. Email: {Saji.Sathyan, Dave.Humphrey, Mark.Hedley}@csiro.au

ready for widespread commercial deployment. As explained in the next section the technology that is most appropriate for terrestrial localization is the time of arrival (TOA) based ranging.

We have developed a WSN platform that we call WASP (Wireless Ad-hoc System for Positioning) that provides accurate TOA-based localization, in addition to wireless communication, using low-cost electronics. In this paper we describe the WASP architecture and the signal processing algorithms, including some novel extensions to existing techniques. A novel TOA estimation algorithm was developed that uses a band-stitching approach to obtain a broadband channel impulse response (CIR) using narrower band electronics. This enables lower cost electronics to be used compared to direct measurement of a broadband CIR. The TOA is computed from the CIR and the algorithm that we have developed [14] is shown to have lower computational complexity compared to other super-resolution algorithms described in the literature. From the TOA the range between node pairs is computed. We also present a novel robust least squares (RLS) localization algorithm that effectively removes outlier range measurements commonly encountered in multipath propagation environments.

The WASP platform has been extensively field tested in a range of radio environments and applications including sports, public safety, and mining with support from government and commercial organizations. This paper presents results from some of the field trials. The results show that WASP provides accurate ranging and localization performance in both indoor and outdoor environments and these results compare favorably with other systems for which published results of evaluations in realistic environments are available.

The rest of this paper is organized as follows. In Section II we describe the challenges faced in developing a low-cost TOA-localization platform, and highlight some existing systems and their limitations. Section III presents the WASP architecture and algorithms that constitute the signal level processing such as TOA estimation and ranging. In Section V the localization and tracking algorithms studied for implementation in the WASP platform are explained. Section VI presents the performance of the system using data collected in field trials. Concluding remarks are given in Section VII.

II. Wireless localization: Challenges and Existing Systems

There are many potential applications for localization and tracking of the nodes in WSNs that are not supported by

current technology. One example is tracking public safety officials such as fire fighters undertaking a mission inside a building. A localization system for this application must provide high accuracy (of the order of one meter) in a wide range of indoor radio propagation environments and be suitable for rapid deployment, yet be small and low cost. These are a challenging set of requirements not fully addressed by any commercial system to date, and a system overcoming these challenges will find use in many other applications including military and mining.

Operation in a wide range of indoor environments requires that the system is robust to fading and severe multipath signals. Unfortunately localization relies on the measurement of direct path distances, so multipath is a problem and cannot be exploited as in communications. Rapid deployment requires that the system does not require prior knowledge of the building, such as maps, or environmental information such as signal strength surveys. It is also not feasible to install any cabled infrastructure in such situations, so all hardware must communicate wirelessly.

There are a number of technologies that are not suitable for this application. Systems using ultrasound (such as the ORL ultrasonic system [37], Cricket [27], and Medusa [32]) or infra-red cannot be used as these signals do not travel through walls. GPS cannot be used as it is generally unavailable indoors. There are other systems that use existing terrestrial infrastructure such as cellular and broadcast television signals, however, their accuracy is typically many tens to hundreds of meters, which is insufficient for this application. A common approach for indoor localization is to use received signal strength (RSS) fingerprints from access points or other in-stalled infrastructure [2], [25], [38]. RSS-based localization is not suitable for rapid deployment as the signal strength survey is slow and requires access to the entire area. Systems based on the measurement of angle of arrival are large (containing steerable antennas or antenna arrays) and provide poor accuracy in multipath environments as the strongest signals are often not the direct signals. This leaves systems based on the measurement of time-of-arrival (TOA) as most suitable for our applications.

There are a number of challenges in obtaining high local-ization accuracy using TOA-based systems. The key challenge is to measure the TOA to an accuracy of the order of one nanosecond using low-cost hardware in difficult radio environments. Another challenge is the time and frequency difference between the local clocks in different nodes. While the use of a cabled infrastructure between anchors – as is used in a number of systems (e.g., Inmotio [16]) – would easily eliminate the synchronization problem, such a system is not feasible for rapid deployment.

Further, the propagation delay through the electronics must be known so that the range is computed from the propagation through the air only. The propagation delay in the electronics, however, varies with parameter settings and temperature. Fig. 1 shows the variation of the propagation delay in a WASP node for different settings of the variable gain amplifier (VGA) on the receiver. It can be seen from the figure that for some VGA settings the excess propagation delay in the hardware is over
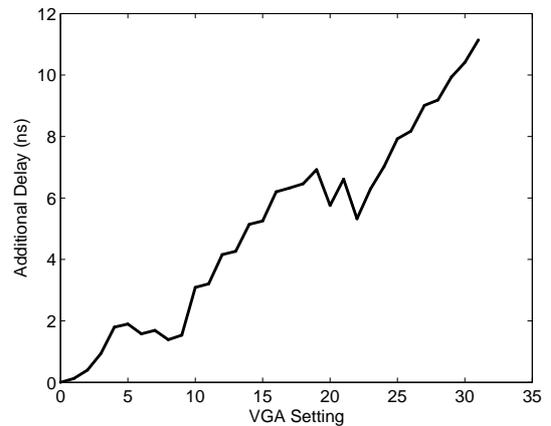

Fig. 1. Variable propagation delay in low-cost hardware as a function of receiver gain.

10 ns, which translates to a ranging error as high as 3 m, if not corrected.

There are few current systems that use TOA for high accuracy ranging and localization. Systems based on UWB [5], [34] have the advantage of high bandwidth, but the low power severely restricts the range of operation and UWB is not yet legal in many jurisdictions outside the USA. The Precision Personnel Locator (PPL) [1] is a research system that seeks to address the specific needs of fire fighters. The PPL is not robust to severe multipath interference and requires two radio subsystems – one for localization and one for data communications – which increases the size, cost, and power consumption. Further, the algorithm used for localization is computationally intensive. Another system addressing similar requirements is presented in [20]. This system overcomes the problem of variable node propagation using a loopback measurement within each node, which is not possible with low-cost radio devices. Further, the results presented in [20] are based on simulations and measurements obtained using precision laboratory equipment; hence, they do not reflect the issues encountered in multipath environments and the use of low-cost hardware.

III. WASP SYSTEM OVERVIEW

A WASP network consists of a number of WASP nodes. Some of these nodes, called anchor nodes, are at known fixed locations, and the rest of the nodes, called mobile nodes, are localized with respect to the anchor node locations. The anchor node locations can be determined using building plans or conventional surveying techniques. For a WASP network that extends outdoors from a building GPS can be used to locate outdoor anchor nodes and WASP can track indoor nodes where GPS is not available.

In typical applications of our system, such as tracking athletes or fire fighters, the anchor nodes surround the area to be monitored and the measured TOA is used to determine range between the mobile and anchor nodes. The mobile nodes are localized and tracked using the measured ranges to the anchors.
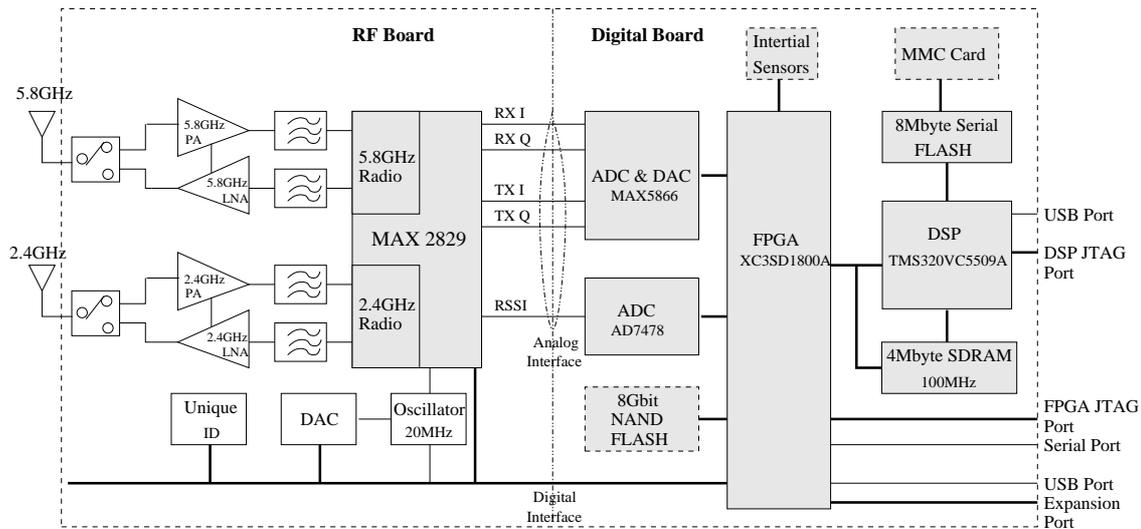
Fig. 2. Node Hardware Architecture.

While the minimum number of anchor nodes for two-dimensional localization is three, we typically deploy between eight and twelve anchor nodes to improve accuracy and to allow for the fact that not all mobiles will be in radio range of all the anchor nodes. Since there is no distinction between the WASP nodes used as mobiles and anchors, a WASP network is also suitable for cooperative localization [24] in which range measurements between mobile nodes permit tracking of mobile nodes that are not within the radio communication range of anchor nodes. While we have undertaken initial research into cooperative localization [31] it has not been required for our applications to date and is not further commented upon in this paper.

A. Radio Spectrum Selection

In WASP we use TOA measurements for ranging. TOA can be determined either by measuring the phase of the received narrowband carrier signal or by measuring directly the arrival time of a narrow wideband pulse [22]. Although the former approach, which is used in real-time kinematic GPS, can give accurate ranging performance outdoors, its performance indoors or in the presence of multipath is significantly degraded. In WASP we use the latter approach.

The accuracy of the TOA measurements, and hence the range, depend upon the bandwidth of the transmitted signal. The standard deviation of the ranging error between a pair of nodes is inversely proportional to the bandwidth of the signal [10]. We found that in typical office buildings a bandwidth of 100 MHz is required to obtain a ranging accuracy of the order of a meter. This observation is consistent with measurements made by other researchers [9].

Due to the prohibitively high cost associated with the use of the licensed spectrum, most of the applications of interest restrict us to use the unlicensed spectrum. We further restrict the operating frequency to be below 10 GHz so that we can use low-cost radio electronics and have reasonable radio propagation through building materials. These restrictions leave us with only the 2.4 GHz and 5.8 GHz ISM (industrial

scientific and medical) frequency bands, which are available internationally and have bandwidths of 83 MHz and 125 MHz respectively. The WASP hardware was built to work in both bands, however, trials to date have used the 5.8 GHz band due to greater bandwidth and less interference from wireless networks.

B. WASP Hardware

The WASP hardware was designed to provide the flexibility and capability to be used as a platform for WSN and localization research, yet also be sufficiently small and low power for field trials. The former was achieved by incorporating much of the functionality in software and firmware, i.e., WASP is a software defined radio system [7].

To design a system that is compact and low-cost we decided to use a highly integrated commodity integrated circuit (IC) for the radio frequency (RF) subsystem. Since no such RF IC existed in the mass market that would provide a bandwidth of up to 125 MHz, we selected a WLAN (wireless local area network) RF IC designed for 802.11 family of protocols. This RF IC, however, does not cover the entire 125 MHz bandwidth, and in our design to utilize the entire bandwidth, the frequency band is divided into eight overlapping subchannels. The division of the bandwidth into subchannels is controlled by software rather than a fixed division in the hardware. The transmitter frequency hops between the subchannels and the receiver stitches the received signals in different subchannels.

An advantage of the narrower band subchannels is the lower sampling rates for the conversion between analog and digital signals, allowing us to use low-cost and low-power components. The disadvantage is that there is increased signal processing complexity at the receiver to stitch together the eight subchannels to reconstruct the full bandwidth signal. The power and cost increase in the digital processing electronics is more than made up for by the reductions in the radio and converter electronics. An example of the processing required for band-stitching is presented in [30].

Fig. 3. Two versions of the WASP node.

Fig. 2 shows a block diagram of our hardware architecture. Most of the radio functions are performed by the Maxim MAX2829 RF IC including conversion between baseband and radio frequency and frequency synthesis. The digital processing is performed by a field programmable gate array (FPGA) for low level processing and a digital signal processor (DSP) for high level processing. A detailed description of the WASP hardware can be found in [10].

Two versions of the WASP hardware are shown in Fig. 3. Both implement the block diagram shown in Fig. 2 and have the same functionality. The larger node, however, has increased connectivity options and a larger battery. The power consumption of the hardware is 2 W while receiving and 2.5 W while transmitting. In high update rate applications such as tracking athletes the battery life between charges is approximately 10 hours and 2.5 hours for the large and small nodes respectively. In low update rate applications active power management can be employed to greatly extend the battery lifetime.

C. Wireless Protocol

Each WASP node periodically transmits a beacon that contains data for network configuration, may contain a user payload, and is used for tracking by measuring the TOA of received beacons. For temporally uniform tracking and accurate measurement of the TOA, the beacons should be regular and contention free and to facilitate this a time division multiple access (TDMA) medium access control (MAC) protocol is used. Time is divided into slots and each node is allowed to transmit in one of the slots. A group of slots is called a superframe, which is a periodically repeating structure.

For tracking athletes we typically use 2.5 ms slots and 40 slots in a superframe of duration 100 ms, providing ten location updates per second for every node. In our system the slot duration and the number of slots in a superframe are configurable and hence, we can make trade offs between the number of active nodes, location update rate, and power consumption to suit each application. As slots are used for anchor nodes and mobile nodes alike, the maximum number of mobile nodes that can be simultaneously tracked is the number of slots in a superframe less the number of anchor nodes.

The MAC provides a distributed mechanism for the allocation of slots to nodes and enables slot reuse for nodes with sufficient separation to be non-interfering. Each node has one slot reserved in each superframe for its beacon, and can also negotiate additional reserved slots for data. Nodes can also send data using a contention access mechanism in unreserved slots. Data packets are transmitted using a single subchannel and beacon packets are data packets that also include a signal designed to enable high accuracy TOA measurement at receivers. This TOA signal includes transmissions on all of the subchannels transmitted sequentially from the lowest subchannel.

The physical layer is similar to that used in 802.11a/g. We use 15 MHz of bandwidth, orthogonal frequency division multiplexing modulation, convolutional encoding, and Viterbi decoding. To ensure high reliability we have used binary phase shift keying and quadrature phase shift keying constellations for data rates of 4 and 8 Mbits/s. The TOA signal consists of identical noise like signals with good correlation properties and 18 MHz bandwidth on each of the subchannels. Each of these has a duration of 41 μs and there is an idle period of 20 μs between transmission on each subchannel to allow the frequency synthesizer to settle to the next carrier frequency.

IV. WASP ALGORITHMS

In each superframe each node transmits a beacon in a specified slot and all nodes measure the TOA of received beacons. The set of beacon transmit and receive times for a superframe is processed to determine the location of mobile nodes. The processing stages consist of performing band-stitching to reconstruct the broadband CIR between each connected pair of nodes, performing super-resolution TOA estimation from the CIR, determining the range between each pair of nodes, and finally performing localization and tracking of the mobile nodes using the measured ranges. Algorithms for TOA and range estimation are described in this section and that for localization and tracking in the following section.

A. TOA Measurement

The bandwidth available to any system is limited by regulatory and hardware restrictions, and this in turn restricts the achievable ranging accuracy of the TOA-based systems. This has prompted several researchers to propose super-resolution TOA measurement techniques that are inspired by similar techniques available for high resolution spectral estimation.

To better understand the similarity between the super-resolution TOA estimation and spectral estimation, consider the multipath channel model

$$h(t) = \sum_{l=0}^{L-1} a_l \delta(t - \tau_l), \qquad (1)$$

where $h(t)$ is the CIR, L is the number of significant multipaths, and a_l and τ_l are, respectively, the complex amplitude and time delay of the lth path. $\delta(.)$ denotes the Dirac delta function.

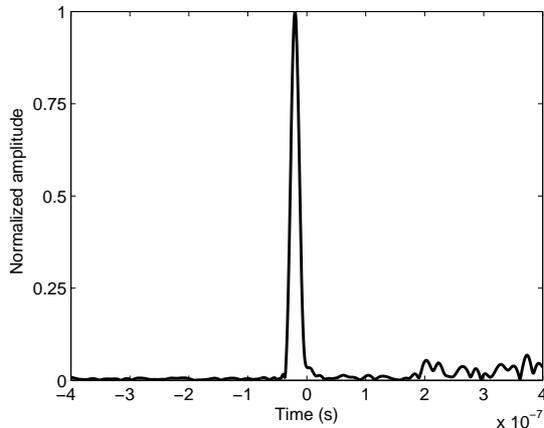Fig. 4. CIR in an outdoor environment showing no significant multipath condition.

Fig. 5. CIR in an indoor environment showing significant multipath condition.

We can obtain the equivalent channel frequency response $H(f)$ by taking the Fourier transform of $h(t)$. Therefore $H(f)$ is given by

$$H(f) = \sum_{l=0}^{L-1} a_l \exp\left(-\jmath\, 2\pi \tau_l f\right). \tag{2}$$

where $\jmath$ denotes the imaginary unit, i.e., $\jmath = \sqrt{-1}$.

If the frequency and time variables in (2) are interchanged, we obtain the classical harmonic signal model. This suggests that the examination of the spectral contents of $H(f)$ will give the multipath amplitudes and delays. It then becomes possible to apply the well-known high-resolution spectral estimation techniques to estimate the TOA.

One of the popular high-resolution spectral estimation techniques ESPRIT (estimation of signal parameters via rotational invariance technique) [26] is used to estimate the TOA in [29]. Variations of the MUSIC (multiple signal classification) algorithm are proposed for TOA estimation in [8] and [18]. In [6], a technique based on the matrix pencil method is proposed. Using simulated channel data the performance of the super-resolution TOA algorithms is compared in [39].

Using the above mentioned super-resolution algorithms is not practical in our system. Even a modest update rate of 2 Hz in a network with 20 nodes requires each node to calculate 40 TOAs per second, i.e., 25 ms per TOA estimation. In sporting applications, higher update rates reduce this to just a few milliseconds per TOA calculation. The super-resolution algorithms mentioned above require the calculation of eigenvalues or inverses of matrices [$\mathcal{O}(M^3)$ complexity for $M \times M$ matrices] with sizes on the order of 100×100 or bigger.

The standard way of determining the TOA, as used in GPS for example, is to estimate the CIR by correlating the received signal against the transmitted signal. An equivalent method to determine the CIR is to multiply $H(f)$ by a window function and then take the inverse Fourier transform. Sample impulse responses measured by our system are shown in Fig. 4 and Fig. 5. Fig. 4 was measured outdoors and shows a clear main peak corresponding to the direct path. Fig. 5 was measured indoors and shows strong multipath propagation.
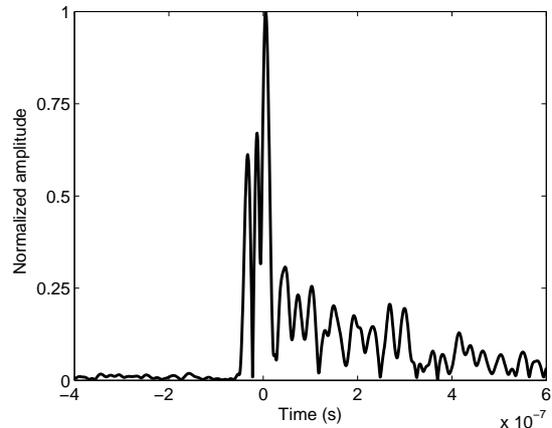
Given the CIR there are numerous ways in which the TOA may be chosen and the exact method has a significant impact on the performance of the system. For the outdoor case the peak of the impulse response is a good choice as in Fig. 4. In indoor or multipath environments such a technique does not work since the strongest peak cannot be used. In this case the direct path may have a lower signal strength than a reflected path. Further, there can be multiple reflected signals overlapping with the direct path signal resulting in the first peak of the combined signal being delayed relative to the peak of the direct path signal. Using a 125 MHz bandwidth signal the pulse width is 16 ns between nulls, and hence, to obtain the desired nanosecond level accuracy a super-resolution approach must be used to find the TOA of the direct path signal.

In our implementation, we choose the TOA as a (small) fixed fraction (-18 dB) of the height of the first peak in the impulse response. This value has been chosen as small as possible while still being reliably above the noise level. As seen in Fig. 8 the noise level is quite constant with respect to the received power level, so an adaptive threshold in not required. By fixing the fraction, the TOA estimate is independent of the amplitude of the first peak, and thus gives good results in the case where the line of sight (LoS) path is the dominant path. By making the fraction as small as possible, this method also has a reasonable chance of picking up the LoS signals that are hidden by more powerful later arriving signals, although the accuracy is reduced.

In our experience, using actual measured data in indoor environments, the performance of the algorithm used in WASP is as good or better than the performance of the MUSIC and ESPRIT super-resolution algorithms, while being vastly simpler to implement [the most complex operation is an FFT with complexity order $\mathcal{O}(M log(M))$]. This contrasts sharply with the simulation only studies of [6], [8], [29] and [39]. It is, however, in line with the results obtained using measured data in [22]. For example, Figures 7 and 9 in [22] show only marginal differences between the results for the MUSIC algorithm and the correlation-based approach. The simulation only studies either use an unrealistically simple channel model,

or use channel models designed for communications which effectively limit the number of paths to the number of degrees of freedom required to represent the channel given the channel bandwidth and the delay spread. These models fail to capture the true range of possible TOAs given a particular CIR. See [14], [15] for a detailed discussion on this point.

We have also investigated a template matching approach based on the shape of the leading edge, which effectively gives a variable threshold. Details of this template matching algorithm along with comparison results can be found in [15].

B. Range Estimation

TOA ranging can use either a one-way or two-way exchange of signals between a pair of nodes. One-way ranging requires synchronization of the clocks of all the anchors and is generally used to estimate pseudo-range, requiring the use of a time difference of arrival (TDOA) localization algorithm. Synchronization errors and the poorer accuracy of TDOA localization algorithms compared to TOA algorithms result in one-way ranging having lower accuracy than two-way ranging, so we focus on the use of two-way ranging.

In two-way ranging, which is also called round-trip ranging [20], as shown in Fig. 6, node A transmits a wideband pulse to node B. After a small delay of τ_{AB}, node B returns a pulse back to node A. In this figure t_i, $i = 1, 2, 3, 4$ denote the absolute times in an unknown time frame common to both nodes. The times shown within brackets denote the corresponding times with respect to the local clocks. The absolute and local times for node n are related by

$$t_i^n = \alpha_n(t_i - t_{0,n}), \qquad (3)$$

where α_n and $t_{0,n}$ are the frequency and time offsets of node n, respectively.

Note that t_1^A and t_3^B are the transmission times at nodes A and B, and are known precisely. t_4^A and t_2^B are the received times at these nodes and are measured by the respective nodes using the super-resolution technique presented in Section IV-A. Knowing these times allows us to calculate the time of flight and the procedure used in WASP is explained in detail in [11]. The procedure corrects for a constant frequency offset between the local clocks in the node pair, and constant relative motion between the node pair. The corrected range between anchor and mobile nodes is determined at the time at which the mobile node transmits. This is done so that in the subsequent localization calculation all ranges between a particular mobile node and the anchor nodes are computed at a common time. Therefore the location of the mobile node is computed at the time at which it transmitted its beacon.

In much of the literature it is assumed that a two-way measurement is between a particular node pair with little delay between the initial beacon and the response, i.e., $\tau_{AB} \approx 0$. For a fully connected network of N nodes there are $N^2/2$ node pairs requiring a total of N^2 transmissions to measure the two-way ranges between all pairs of nodes. In WASP each node only transmits once for a total of N transmissions. The reduction in the number of transmissions leads to a more power efficient and higher location update rate system. The downside
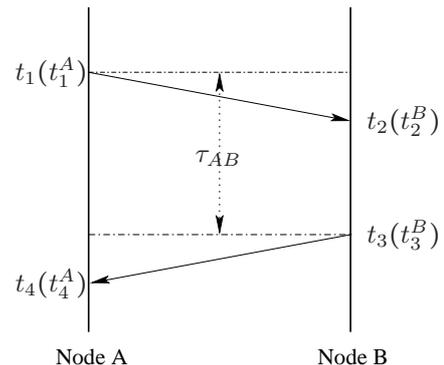

Fig. 6. The two-way range between a pair of nodes A and B is measured using an exchange of signals between each nodes.

is the substantial time delay between the two beacons of a node pair and the processing algorithms must allow for factors such as node motion and node clock frequency differences in this interval.

V. LOCALIZATION AND TRACKING ALGORITHMS

It is necessary to consider different techniques for localization in indoor and outdoor environments because of the varying propagation conditions of these environments. We compare three localization algorithms including a new robust least squares (RLS) technique that we have developed. The robust technique removes the outlier range measurements effectively and compared to the standard LS technique gives improved localization accuracy.

The positioning accuracy can be further improved by tracking the node. Tracking also allows the estimation of kinematic parameters such as velocity and acceleration. In this paper we consider two tracking approaches. In the first approach the positions obtained in the localization step are used in a Kalman filtering framework to track the nodes. In the second approach the localization step is removed altogether and the range measurements are fused directly using a nonlinear filter.

A. Localization Algorithms

We compared three localization algorithms: the standard LS, the new RLS, and the projection onto convex sets (POCS). In this section we provide a brief description of the standard LS and POCS algorithms and the details of the RLS algorithm.

1) Least Squares Algorithm: Assume that the measured range between unknown node and the anchor i is given by

$$r_i = \| \boldsymbol{\theta} - \boldsymbol{\theta}_i \| + w_i \qquad i = 1, 2, \ldots, N \qquad (4)$$

where N is the number of anchors in the network, $\boldsymbol{\theta} = [x, y]^T$ is the unknown location of the node, and $\boldsymbol{\theta}_i = [x_i, y_i]^T$ is the known location of the ith anchors. w_i is the range measurement noise, which is assumed to have a zero mean and σ_i^2 variance and $\| . \|$ denotes the two-norm.

The well-known LS technique minimizes the sum of the square of the difference between the measured and estimated ranges or in other words the range noise power [19]. The LS

estimate of the unknown node location $\boldsymbol{\theta} = [x, y]^T$ is then given by

$$\hat{\boldsymbol{\theta}}_{LS} = \arg\min_{\boldsymbol{\theta}} \sum_{i=1}^{N} \left(r_i - \| \boldsymbol{\theta} - \boldsymbol{\theta}_i \| \right)^2 \quad (5)$$

The minimization problem in (5) is nonlinear and a closed form solution is not available. It can be solved using any gradient descent techniques. In this paper we used the iterative LS algorithm, which is based on a Taylor series expansion of the objective function [3]. The gradient descent type algorithms require a starting point close to the actual solution. Otherwise, they may converge to a local minima or may not converge at all. For localization using ranging, an initial solution can be easily obtained using a linear approximation as explained in [33]. If the node is being tracked the prior track information can be used as well.

2) Robust Least Squares (RLS) Algorithm: The standard LS algorithm just described uses all the range measurements irrespective of their quality.[1] In this paper we propose a robust algorithm that tries to remove outlier measurements through an iterative process.

In the RLS algorithm, first we compute the node location using the LS technique and the corresponding positioning error [see (6)] based on all the N range measurements. Then we remove each measurement in turn, and recompute the node position and the corresponding positioning error. The measurement, which when removed gives the smallest positioning error, is identified and after applying a small bias towards using more measurements, if the positioning error is still smaller, the removed measurement is considered an outlier and eliminated from further consideration. This process is repeated until an acceptable positioning error is obtained.

The positioning error is calculated as the product of the geometric dilution of precision (GDOP) and the ranging error. That is

$$e = \text{GDOP} \sqrt{\sum_{i=1}^{N} \frac{\left(r_i - \| \hat{\boldsymbol{\theta}}_{LS} - \boldsymbol{\theta}_i \| \right)^2}{N - 2}}. \quad (6)$$

In the above $\text{GDOP} = \sqrt{\text{trace}(AA')^{-1}}$, where $'$ denotes the matrix transpose and the matrix A is given by

$$A = \begin{bmatrix} \frac{x-x_1}{\|\boldsymbol{\theta}-\boldsymbol{\theta}_1\|} & \frac{x-x_2}{\|\boldsymbol{\theta}-\boldsymbol{\theta}_2\|} & \cdots & \frac{x-x_N}{\|\boldsymbol{\theta}-\boldsymbol{\theta}_N\|} \\ \frac{y-y_1}{\|\boldsymbol{\theta}-\boldsymbol{\theta}_1\|} & \frac{y-y_2}{\|\boldsymbol{\theta}-\boldsymbol{\theta}_2\|} & \cdots & \frac{y-y_N}{\|\boldsymbol{\theta}-\boldsymbol{\theta}_N\|} \end{bmatrix}. \quad (7)$$

Calculation of the positioning error e is based on the simplifying assumption that the noise in the range measurements is independent and Gaussian distributed, which while not strictly true was found to work well with real data. A pseudo-code description of the RLS algorithm is presented in Table I.

The selection of the optimal bias κ is dependent upon the statistics of the range errors, however, we have found in practice that a wide range of values provide acceptable performance. Fig. 7 shows this using real data collected by WASP in a velodrome, where the LoS measurements are available

---

[1]A weighted LS algorithm can be envisaged to incorporate measurement quality. If the measurement noise is Gaussian distributed, then the optimal weights are the inverse of the measurement noise variances. Finding the optimal weights for other distributions, however, may not be feasible.

TABLE I
THE ROBUST LEAST SQUARES (RLS) ALGORITHM

Calculate node location $\boldsymbol{\theta}_N$ using NLS algorithm from N measurements
Calculate corresponding location error e_N using (6)
repeat
  for all anchor $i \in N$ **do**
    Remove r_i from the measurement set
    Calculate node location $\boldsymbol{\theta}_{N/i}$
    Calculate corresponding location error $e_{N/i}$
    Store $(i, \boldsymbol{\theta}_{N/i}, e_{N/i})$
  end for
  if $\min_i \kappa e_{N/i} < e_N$, {$\kappa$ is the bias} **then**
    Remove r_i from the measurement set
    Set $N = N - 1$
    Set $\boldsymbol{\theta}_N = \boldsymbol{\theta}_{N/i}$
    Set $e_N = \min_i e_{N/i}$
  else
    break
  end if
until $e_{N/i} \leq$ a given threshold
return $\boldsymbol{\theta}_N$

Note: In the above N/i denotes all indexes from 1 to N except i, i.e., $1, 2, \ldots, i-1, i+1, \ldots, N$.
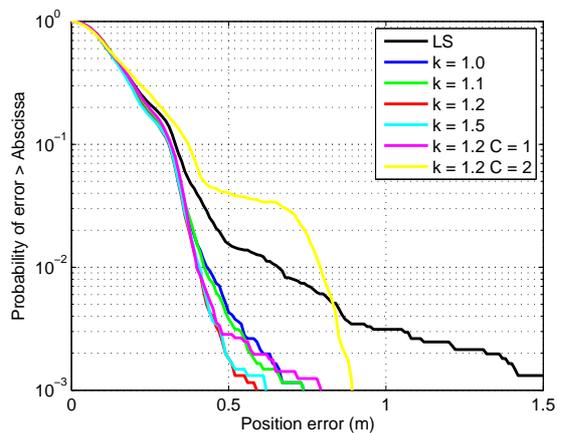

Fig. 7. Complementary cumulative distribution function for position error using velodrome data. In all cases, except standard LS, RLS was used for positioning with κ given in the legend. C, the number of range measurements in each data set artificially corrupted to create outliers, is zero unless stated otherwise in the legend.

but severe multipath is present due to the metal structures and building enclosure. Multiple measurements were made at each of the 15 surveyed locations, for a total of 6077 sets of measurements for localization, where each set contains the range to at most nine anchors. It is seen that while $\kappa = 1.2$ provides the lowest error, values between 1.0 and 1.5 provide satisfactory performance, which is significantly better than the standard LS technique.

To further demonstrate the performance of our robust algorithm using the same data we corrupted one or two range measurements in each set by adding a uniformly distributed random noise in the range [-10,10] m. The results are also shown in Fig. 7 and these cases are denoted in the legend by C = 1 and C = 2 for one and two large outliers, respectively. It is seen that with one range outlier there is little additional error, and that even with two outliers nearly 95% of the position values have little additional error. The LS technique failed to converge for all measurement sets even with a single outlier.

These results show the substantial improvement that can be obtained using our RLS algorithm.

3) Projection onto Convex Sets (POCS) Algorithm: The POCS algorithm was proposed for localization in [12]. Unlike the LS technique where the error between measured and estimated range is penalized quadratically, the POCS algorithm applies a penalty only when the estimated range is greater than the measured range. As a result this algorithm can provide better results when the range measurements have large positive biases, which typically is the case in strong multipath environments.

In the POCS algorithm, each range measurement is used to form a convex constraint on the unknown node position. With range measurements the convex set is defined by

$$D_i = \left\{ \boldsymbol{\theta} \in \mathbb{R}^2 \; ; \; \| \boldsymbol{\theta} - \boldsymbol{\theta}_i \| \leq r_i \right\}, \quad i = 1, 2, \cdots, N. \quad (8)$$

This effectively transforms the localization problem into a convex feasibility problem [12]. That is

$$\hat{\boldsymbol{\theta}}_{POCS} = \bigcap_{i=1}^{N} D_i \in \mathbb{R}^2. \quad (9)$$

Starting from a random initial point, for each constraint, if the constraint is not satisfied the point is updated by projecting it onto the convex set defined by that constraint. Given that the intersection set is non-empty, this process is guaranteed to converge to a feasible point [12]. In our implementation of the POCS algorithm, we used a number of different starting points and the algorithm is allowed to run for a fixed number of iterations for each starting point. The resulting points are averaged to obtain the position of the unknown node. This procedure gives the approximate centroid of the intersection region.

B. Tracking Localized Nodes

The localization accuracy of the algorithms considered can be improved by applying a filtering algorithm on the estimated nodes positions. Let $\mathbf{x}_k = [x_k, \dot{x}_k, \ddot{x}_k, y, \dot{y}_k, \ddot{y}_k]^T$ be the state vector at time k, where (x, y), $(\dot{x}, \dot{y})$, and $(\ddot{x}, \ddot{y})$, respectively, are the position, velocity, and acceleration components in the x and y directions. If we assume that the node dynamics is adequately represented using a linear motion model, then the state equation can be written as

$$\mathbf{x}_{k+1} = F_k \mathbf{x}_k + \nu_k \quad (10)$$

where F_k is the state transition matrix and ν_k the process noise, which is assumed to be a white Gaussian sequence having covariance Q_k. Since the localized node position is considered as the measurement, the measurement equation is given by

$$\mathbf{z}_{k+1} = H \mathbf{x}_{k+1} + \omega_{k+1} \quad (11)$$

where H is the measurement matrix given by

$$H = \begin{bmatrix} 1 & 0 & 0 & 0 & 0 & 0 \\ 0 & 0 & 0 & 1 & 0 & 0 \end{bmatrix} \quad (12)$$

and ω_{k+1} is the measurement noise, which is the localization error. In our implementation since the covariance of ω_{k+1} is

not known, following [23], we used the Cramér-Rao lower bound (CRLB) instead.

Since the state-space model defined by (10) and (11) is linear, the well-known Kalman filter (KF) can be used to track the localized nodes, details of which can be found in numerous texts including [3].

C. Direct Fusion of Range Measurements

Another approach one could take to track a node is the direct fusion of the range measurements using filtering techniques without explicit localization of the node as a prior step. One reason for considering this approach is that when there are outlier range measurements, the localization step could amplify it, leading to reduced tracking performance.

In this approach the state model remains the same as in (10). The range measurements of all the anchors at a given time are used to form a measurement vector $\mathbf{r}_k = [r_1, r_2, \cdots, r_N]^T$. Then the following measurement model is easily obtained.

$$\mathbf{r}_{k+1} = h(\mathbf{x}_{k+1}) + \mathbf{w}_{k+1} \quad (13)$$

where $h(.)$ is the measurement function given by

$$h(\mathbf{x}_k) = \begin{bmatrix} \sqrt{(x - x_1)^2 + (y - y_1)^2} \\ \sqrt{(x - x_2)^2 + (y - y_2)^2} \\ \vdots \\ \sqrt{(x - x_N)^2 + (y - y_N)^2} \end{bmatrix} \quad (14)$$

and $\mathbf{w}_{k+1} = [w_{1,k+1}, w_{2,k+1}, \ldots, w_{N,k+1}]^T$ is the range noise vector having covariance matrix $R = \text{diag}(\sigma_1^2, \sigma_2^2, \ldots, \sigma_N^2)$.

With the nonlinear state space model defined by (10) and (13), a nonlinear filter is required for state update on the arrival of a new set of measurements.

A number of nonlinear filtering algorithms are available for state estimation [28]. The extended KF (EKF) uses a Taylor series expansion to linearize the nonlinear model, and propagates the mean and covariance of the state through the linearized state-space model [3]. The unscented KF (UKF) uses a deterministic sampling approach in which the state is represented by carefully chosen sample points [17]. These points are propagated through the nonlinear system without any linearization of the state space model as in the EKF. It has been shown that the UKF can perform better that the EKF [36]. Further, the UKF does not require the calculation of Jacobian or the Hessian of the nonlinear state-space functions. Hence, we selected the UKF for the direct fusion of the WASP measurements.

1) Multiple Model Estimation: The range measurement noise characteristics are dependent on the radio propagation environment. Therefore unless a measurement campaign is conducted before the deployment of the system, the range noise characteristics such as the variance σ_i^2 is not known a priori. And as mentioned before for applications that require rapid deployment such an approach is not suitable.

In this paper we consider an alternate approach in which a multiple model estimation, where the measurement is characterized by not one but several measurement models each having different noise variance, is used. The well-known interacting multiple model (IMM) estimator [3] can then be used to update the node state.
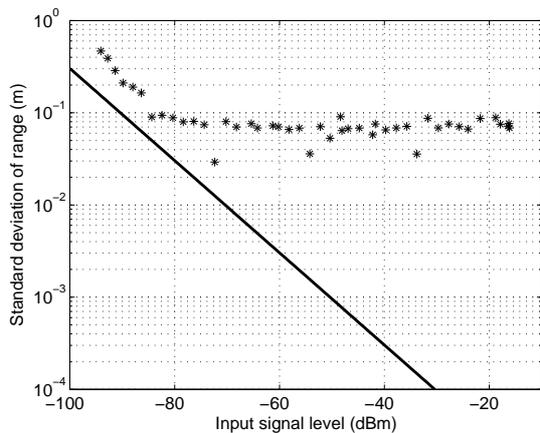
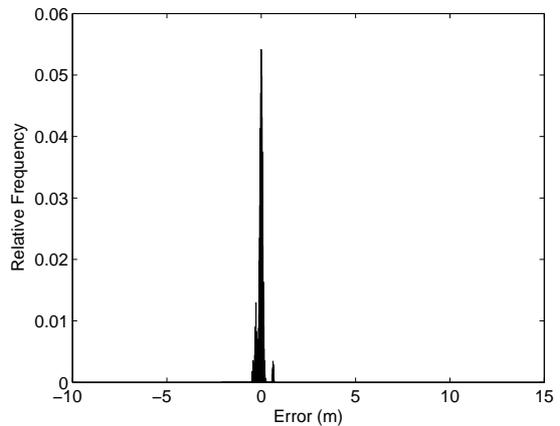Fig. 8. Measured standard deviation of ranging error and the Cramér-Rao lower bound.

Fig. 9. Range error distribution between anchors and the nodes in the soccer field trial.

VI. System Performance

We performed extensive field trials to evaluate the performance of WASP. In this section we first present the ranging accuracy of WASP in different environments and then present the results of the localization and tracking algorithms described in the previous section.

A. Ranging Performance

1) Ideal Conditions: We first evaluated the ranging performance of WASP under ideal conditions by connecting two nodes using cables. The performance of the system at different input signal levels was measured and the standard deviation of the ranging errors is shown in Fig. 8, along with the CRLB on the TOA estimation. The CRLB is given by [35]

$$\sigma_r^2 \geq \frac{1}{8\pi^2 \gamma \text{BW}^2} \qquad (15)$$

where γ is the signal-to-noise ratio (SNR) and BW is the bandwidth of the signal. These measurements were made at 5.8 GHz and WASP has a bandwidth of 125 MHz at this frequency of operation. The SNR is calculated assuming thermal noise and a receiver noise figure of 5 dB.

One can observe from Fig. 8 that the ranging performance of WASP is not affected by the input signal level as long as it is above -85 dBm.[2] When the input signal is above this level, there exists a noise floor of nearly 7 cm. This floor is due to other sources of error that are independent of the input signal level, including noise in the baseband electronics, quantization noise in the converters, and phase noise in the oscillator.

2) Outdoor Trial - Soccer Field: In this trial nine anchors were placed on the periphery of the soccer field and five nodes were placed on the centerline. The true positions of the anchors and the nodes were obtained through a field survey with the center of the soccer field as the origin. In this trial the TDMA frame consisted of 20 time slots each having a duration of 4 ms. In every frame each anchor transmits once and each node
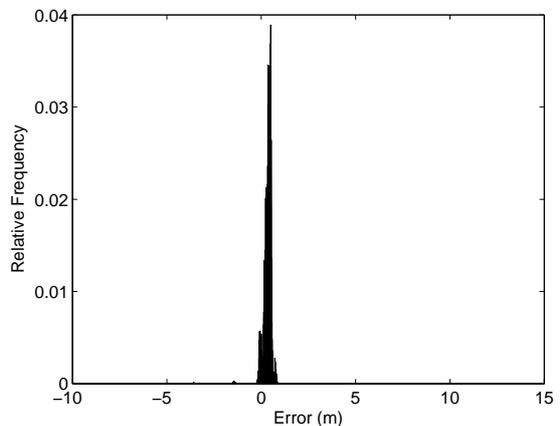

Fig. 10. Range error distribution between anchors and the nodes in the indoor LoS trial.

transmits twice. This gives a location update rate of 25 Hz for each node.

Fig. 9 shows the range error distribution obtained in this trial. One can see that in this trial the WASP provides high ranging accuracy, with nearly 85% of the ranging errors are less than 15 cm.

3) Indoor LoS Trial: This trial was conducted in a large room in a sporting facility building with metal cladding. The room is used for performance monitoring of athletes and consisted of several apparatuses with metal structures. Similar to the outdoor trial nine anchors and five static nodes were used with the same TDMA frame structure. The anchors were placed roughly in a circle of radius 10 m, and five nodes were placed inside the circle in a straight line at 1 m separation.

The range error distribution is shown in Fig. 10. The distribution shows a positive bias in the errors. This indicates a multipath condition inside the laboratory. Of all the ranging errors 82% are less than 0.5 m.

4) Indoor NLoS Trial: This trial was conducted inside a regular office building. The building layout and the node locations are shown in Fig. 11. The internal walls consisted of a mix of plasterboard, reinforced concrete, metal frames, and
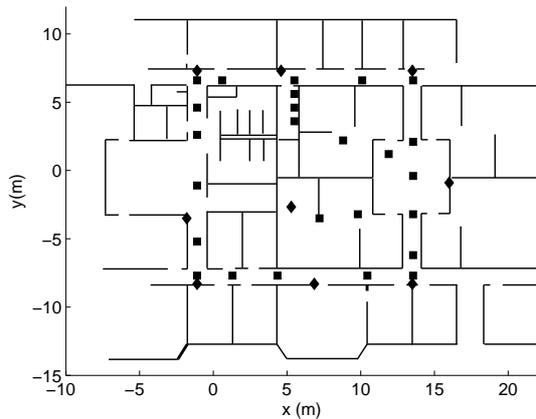
---

[2]An RF input signal level of -85 dBm corresponds to a range of nearly 200 m for our system in free space.

Fig. 11. Node placement in the indoor NLoS trial. Anchors are denoted by ◆ and node locations by ■.
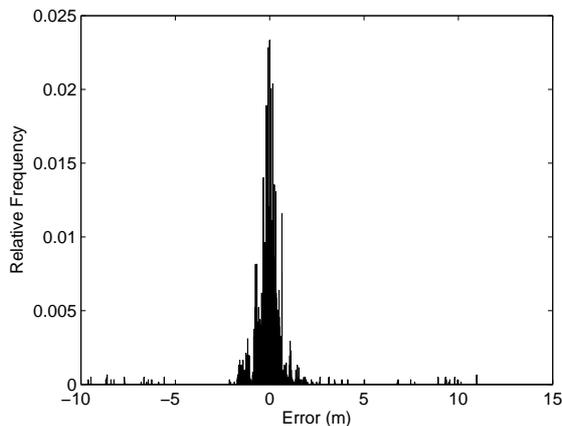

Fig. 12. Range error distribution between anchors and the nodes in the indoor NLoS trial.

glass. In this trial nine WASP nodes were placed at surveyed locations and assumed as the anchor nodes. Another node was placed at various locations throughout the building as shown in the figure and was localized. At each location of the node several ranging measurements were obtained. From the layout it is easy to see that for most pairs of nodes the LoS path is blocked by the walls and partitions inside the building.

The range error distribution for this case is shown in Fig. 12. Observe from the figure that there is a considerable probability mass away from the main cluster. In this trial only 65% of the ranging errors are less than 0.5 m.

B. Localization Performance

The localization performance of WASP was evaluated in both static and dynamic scenarios. As we had no independent system for high accuracy tracking of nodes, evaluation of location error was only possible by using the surveyed locations of static nodes. For this the measurements collected in Sections VI-A2, VI-A3, and VI-A4 were used. In a dynamic scenario, however, only the evaluation of relative location error is possible, where two nodes are constrained to have a fixed

TABLE II
RMS LOCALIZATION ERROR (CM) — STATIC SCENARIO

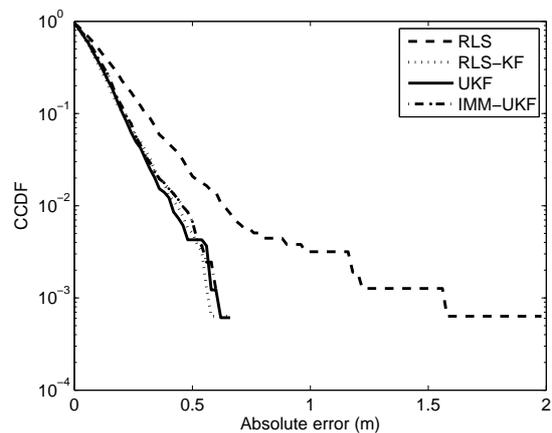| Trial	LS	RLS	POCS	KF	UKF	IMM/UKF
Outdoor	12.1	12.0	19.7	11.23	11.9	11.9
Indoor LoS	21.2	16.3	24.1	14.0	18.1	17.9
Indoor NLoS	89.1	68.8	61.0	66.2	74.1	65.8

Fig. 13. Complementary cumulative distribution function of relative location error in the dynamic trial.

separation. Using the estimated locations of the two nodes, the separation error was calculated.

1) Static Trials: Table II shows the root mean square (RMS) localization error performance obtained using different localization algorithms. The POCS algorithm only penalizes range measurements that are less than the estimated range. Hence, in NLoS environments, where biased range measurements are expected, the POCS algorithm is seen to perform the best. The results also show that compared to the standard LS algorithm the proposed RLS algorithm reduces the RMS error by 20.3 cm, because it effectively removes the outlier measurements. The IMM estimator performs better compared to the UKF in NLoS environments because it better captures the varying noise characteristics through the use of multiple measurement models.

In the outdoor data, ranging errors are dominated by system noise and there is no significant bias present. In this case the LS techniques, which use a quadratic penalty function, performs much better than the POCS algorithm. In the indoor LoS case, multipath reflections, although not as severe as in the NLoS case, still causes large outliers. Again the advantage of using the new RLS algorithm over standard LS algorithm can be clearly seen, nearly 23% reduction in RMS location error.

2) Dynamic Trial: We conducted a dynamic trial in which a cyclist was tracked in a velodrome. Two nodes were fixed to the bicycle at a separation of 0.7 m and nine anchors were setup around the velodrome track. Using the range measurements obtained at these nine anchors each node is tracked independently using the two tracking approaches considered. The complementary cumulative distribution of the separation error, i.e., the difference between the true and the calculated

TABLE III
PERFORMANCE COMPARISON WITH OTHER SYSTEMS. (μ_r - MEAN RANGING ERROR, μ_p - MEAN LOCATION
ERROR, AND P_e - PROBABILITY OF RANGING ERROR)

Ref.	Environment	BW (MHz)		Performance	
		Ref.	WASP	Ref.	WASP
[9]	Steel and LoS	500	125	μ_r = 66 cm	μ_r = 38 cm
[9]	Sheet rock/aluminum stud, NLoS	500	125	μ_r = 91 cm	μ_r = 48 cm
[4] [a]	Several buildings, NLoS	100	125	60%, P_e < 3 m	65%, P_e < 0.5 m
[1] [b]	Wood building, NLoS	150	125	μ_p = 0.49 m	0.49 m
[25]	Office building, NLoS	40	125	RMSE = 1.23 m	RMSE = 0.61 m

[a]The results presented in [4] were based on measurements collected at three different sites, which are made of different materials. The corresponding figure presented for WASP is based on the setup described in Section VI-A4.

[b]The measurements are obtained using a system similar to WASP (differences between the two are described in Section II). The corresponding performance measure quoted for WASP is the median error. But this was obtained in an office building with multiple walls and not all of them are made of wood.

separation, is shown in Fig. 13.

It can be seen from the figure that nearly all the probability mass of the separation error is less than 0.5 m for both the direct fusion algorithms. RLS denotes the localization performance obtained using the proposed robust LS algorithm before applying any filtering. When a KF is applied on the localized data, the separation error obtained, shown by the RLS-KF curve in the figure, reduces significantly and is comparable to that obtained using the direct fusion approach.

C. Comparison to Existing Systems

While most publications in this field report simulation results, there are some groups that have performed and reported measurements using real systems. In this section we compare our results with some of those previously reported. In all cases we use our data set that most closely matches their measurement environment. The results are summarized in Table III. When interpreting the results, one should take into consideration that neither the radio parameters nor the environmental conditions were the same.

The first three results in Table III evaluate the ranging accuracy and in all three cases expensive laboratory equipment such as network analyzers is used to perform ranging. Therefore they do not have the additional issues such as time and frequency synchronization that we encounter in using low-cost wirelessly connected nodes, nonetheless our results are generally better. Further, compared to [9] we have only one quarter the bandwidth available for ranging.

The last two comparisons are of localization error. In both [1] and [25] the performance of these systems and our system are similar, taking into account the radio bandwidth available. As mentioned before, compared to [1] WASP has the advantage that it uses a single radio for both positioning and data communication, reducing the cost and power consumption. [25] uses Data ExacTime GPS and rubidium-based oscillators to time synchronize the nodes, which are neither small nor low-cost.

VII. CONCLUSIONS

In this paper we presented a localization system that we have developed called WASP, and field trials to validate its performance across a number of applications. The system was designed to permit rapid setup and to provide high accuracy localization using low-cost hardware, as well as providing high rate data communications. The hardware was designed to be small and low-power, yet with sufficient processing capability to be used for both wireless sensor network (WSN) research and application trials. The sophisticated signal processing algorithms that form part of the system overcome many of the hardware limitations including lack of time and frequency synchronization between nodes, varying propagation delay through the node electronics, and bandwidth limitations of the low-cost RF electronics. New algorithms were presented for super-resolution measurement of TOA and for localization in LoS and NLoS environments.

WASP has been field tested in a variety of scenarios and the results show that WASP can achieve ranging error less than 0.15 m outdoors. In indoor environments where LoS is present, WASP achieves better than 0.5 m accuracy 85% of the time and in NLoS environments the same error figure is achieved 65% of the time. The RMS localization error of WASP varies from 0.11 m to 0.61 m across these environments.

Trials to date have included tracking elite athletes in a range of sports and tracking vehicles in mines. In these applications localization is based on ranging between each mobile node and multiple anchor nodes. WASP hardware and protocols are also suitable for cooperative localization in which the use of range measurements between mobile nodes permits tracking of nodes that are not within the radio communication range of three or more anchors. We are undertaking research into cooperative localization, particularly to reduce the number of anchor nodes required in large networks. We are also undertaking continuing research to improve the performance of the TOA estimation, localization, and tracking algorithms across a wide range of applications.

REFERENCES

[1] V. Amendolare, D. Cyganski, R. J. Duckworth, S. Makarov, J. Coyne, H. Daempfling, and B. Woodacre, "WPI precision personnel location system: Inertial navigation supplementation," in *Proc. Position Location And Navigation Symposium*, Monterey, CA, May 2008, pp. 350–357.

[2] P. Bahl and V. Padmanabhan, "RADAR: an in-building RF-based user location and tracking system," in *Proc. Nineteenth Annual Joint Conference of the IEEE Computer and Communications Societies*, vol. 2, Tel Aviv, Isreal, Mar. 2000, pp. 775–784.

[3] Y. Bar-Shalom, X. R. Li, and T. Kirubarajan, *Estimation with Applications to Tracking and Navigation*. New York, NY: John Wiley & Sons, 2001.

[4] J. Beneat, K. Pahlavan, and P. Krishnamurthy, "Radio channel characterization for geolocation at 1GHz, 500MHz, 90MHz and 60MHz in suo/sas," in *Proc. IEEE Military Communications Conf.*, Atlantic City, NJ, 1999, pp. 1060–1063.

[5] A. Conti, D. Dardari, and M. Z. Win, "Experimental results on cooperative UWB based positioning systems," in *Proc. IEEE Int'l Conf. on Ultra Wideband*, vol. 1, Hannover, Germany, 2008, pp. 191–195.

[6] N. Dharamdial, R. Adve, and R. Farha, "Multipath delay estimations using matrix pencil," in *Proc. IEEE Wireless Communications and Networking Conf.*, vol. 1, New Orleans, LA, Mar. 2003, pp. 632–635.

[7] M. Dillinger, K. Madani, and N. Alonistioti, Eds., *Software Defined Radio: Architectures, Systems, and Functions*. West Sussex, England: John Wiley & Sons, 2003.

[8] F. Ge, D. Shen, Y. Peng, and V. O. K. Li, "Super-resolution time delay estimation in multipath environments," *IEEE Trans. Circuits Syst. I*, vol. 54, no. 9, pp. 1977–1986, Sep. 2007.

[9] C. Gentile and A. Kik, "An evaluation of ultra wideband technology for indoor ranging," in *Proc. IEEE Global Telecommunications Conf.*, San Francisco, CA, Nov. 2006, pp. 1–6.

[10] M. Hedley, P. Ho, D. Humphrey, A. Kajan, A. Grancea, and J. Pathikulangara, "A platform for radio location research in ad hoc and sensor networks," in *Proc. IEEE Int'l Symp. on Communications and Information Technologies*, Sydney, Australia, Oct. 2007, pp. 876–881.

[11] M. Hedley, D. Humphrey, and P. Ho, "System and algorithms for accurate indoor tracking using low-cost hardware," in *Proc. Position Location And Navigation Symposium*, Monterey, CA, May 2008, pp. 633–640.

[12] A. O. Hero III and D. Blatt, "Sensor network source localization via projection onto convex sets (POCS)," in *Proc. IEEE Int'l Conf. on Acoustics, Speech, and Signal Processing*, vol. 3, Philadelphia, PA, Mar. 2005, pp. iii/689–iii/692.

[13] B. Hofmann-Wellenhof, H. Lichtenegger, and J. Collins, *Global Positioning System: Theory and Practice*, 4th ed. New York, NY: Springer-Verlag, 1997.

[14] D. Humphrey and M. Hedley, "Super-resolution time of arrival for indoor localization," in *Proc. IEEE Int'l Conf. Communications*, Beijing, China, May 2008, pp. 3286–3290.

[15] ——, "Prior models for indoor super-resolution time of arrival estimation," in *Proc. IEEE VTC Spring Conf.*, Barcelona, Spain, 2009, pp. 1–5.

[16] (2009) Inmotio local positioning measurement system. Inmotio. [Online]. Available: http://www.inmotio.nl/

[17] S. J. Julier and J. K. Uhlmann, "Unscented filtering and nonlinear estimation," *Proc. IEEE*, vol. 92, no. 3, pp. 401–422, Mar. 2004.

[18] X. Li and K. Pahlavan, "Super-resolution TOA estimation with diversity for indoor geolocation," *IEEE Trans. Wireless Commun.*, vol. 3, no. 1, pp. 224–234, Jan. 2004.

[19] H. Liu, H. Darabi, P. Banerjee, and J. Liu, "Survey of wireless indoor positioning techniques and systems," *IEEE Trans. Syst., Man, Cybern. C*, vol. 37, no. 6, pp. 1067–1080, Nov. 2007.

[20] D. McCrady, L. Doyle, H. Forstrom, T. Dempsey, and M. Martorana, "Mobile ranging using low-accuracy clocks," *IEEE Trans. Microw. Theory Tech.*, vol. 48, no. 6, pp. 951–958, Jun 2000.

[21] L. Ni, Y. Liu, Y. C. Lau, and A. Patil, "LANDMARC: Indoor location sensing using active RFID," in *Proc. IEEE Int'l Conf. on Pervasive Computing and Communications*, Fort Worth, TX, Mar. 2003, pp. 407–415.

[22] K. Pahlavan, X. Li, and J.-P. Makela, "Indoor geolocation science and technology," *IEEE Commun. Mag.*, vol. 40, no. 2, pp. 112–118, Feb. 2002.

[23] K. R. Pattipati, R. L. Popp, and T. Kirubarajan, "Survey of assignment techniques for multitarget tracking," in *Multisensor-Multitarget Tracking: Applications and Advances*, Y. Bar-Shalom and W. D. Blair, Eds. Boston, MA: Artech House, 2000, vol. 3.

[24] N. Patwari, J. N. Ash, S. Kyperountas, A. O. Hero III, R. L. Moses, and N. S. Correal, "Locating the nodes: Cooperative localization in wireless sensor networks," *IEEE Signal Process. Mag.*, vol. 22, no. 4, pp. 54–69, Jul. 2005.

[25] N. Patwari, A. O. Hero III, M. Perkins, N. S. Correal, and R. J. O'Dea, "Relative location estimation in wireless sensor networks," *IEEE Trans. Signal Process.*, vol. 51, no. 8, pp. 2137–2148, Aug. 2003.

[26] A. Paulraj, R. Roy, and T. Kailath, "Estimation of signal parameters via rotational invariance techniques – ESPRIT," in *Proc. Asilomar Conf. on Circuits, Systems, and Computers*, Pacific Grove, CA, Nov. 1995, pp. 83–89.

[27] N. B. Priyantha, A. Chakraborty, and H. Balakrishnan, "The cricket location-support system," in *Proc. IEEE Int'l Conf. Mobile Computing and Networking*, Boston, MA, 2000, pp. 32–43.

[28] B. Ristic, S. Arulampalam, and N. Gordon, *Beyond the Kalman Filter: Particle Filters for Tracking Applications*. Artech House, 2004.

[29] H. Saarnisaari, "TLS-ESPRIT in a time delay estimation," in *Proc. IEEE Vehicular Technology Conf.*, Phoenix, AZ, May 1997, pp. 1619–1623.

[30] E. Saberinia and A. H. Tewfik, "Enhanced localization in wireless personal area networks," in *Proc. of IEEE Global Telecommunications Conf.*, vol. 4, Dallas, TX, Dec. 2004, pp. 2429–2434.

[31] T. Sathyan and M. Hedley, "Evaluation of algorithms for cooperative localization in wireless sensor networks," in *Proc. IEEE Personal, Indoor and Mobile Radio Conference, presented*, Tokyo, Japan, Sep. 2009.

[32] A. Savvides, H. Park, and M. B. Srivastava, "The bits and flops of the n-hop multilateration primitive for node localization problems," in *Proc. 1st ACM International Workshop on Wireless Sensor Networks and Application*, Atlanta, GA, Sep. 2002, pp. 112–121.

[33] A. Sayed, A. Tarighat, and N. Khajehnouri, "Network-based wireless location: challenges faced in developing techniques for accurate wireless location information," *IEEE Signal Process. Mag.*, vol. 22, no. 4, pp. 24–40, Jul 2005.

[34] N. O. Tippenhauer and S. Capkun, "UWB-based secure ranging and localization," ETH, Zurich, Switzerland, Tech. Rep., 2008.

[35] H. Urkowitz, *Signal Theory and Random Processes*. Dedham, MA: Artech House, 1983.

[36] E. A. Wan and R. Van Der Merwe, "The unscented Kalman filter for nonlinear estimation," in *Proc. IEEE Adaptive Systems for Signal Processing, Communications, and Control Symposium*, Lake Louise, AB, Canada, Oct. 2000, pp. 153–158.

[37] A. Ward, A. Jones, and A. Hopper, "A new location technique for the active office," *IEEE Personal Communications*, vol. 4, no. 5, pp. 42–47, Oct. 1997.

[38] M. Youssef, A. Agrawala, and A. Udaya Shankar, "WLAN location determination via clustering and probability distributions," in *Proc. First IEEE Int'l Conf. on Pervasive Computing and Communications*, Mar. 2003, pp. 143–150.

[39] F. Zhao, W. Yao, C. C. Logothetis, and Y. Song, "Super-resolution TOA estimation in OFDM systems for indoor environments," in *Proc. IEEE Int'l. Conf. Networking, Sensing and Control*, vol. 4, London, UK, Apr. 2007, pp. 723–728.

Thuraiappah Sathyan (S'04-M'08) was born in Jaffna, Sri Lanka. He received the B.Sc.Eng. degree from the University of Peradeniya, Sri Lanka in 2001, and the M.A.Sc. and Ph.D. degrees from the McMaster University, Canada in 2004 and 2008, respectively. From January 2001 to December 2002, he was a lecturer in the Department of Electrical and Electronic Engineering at the University of Peradeniya. Currently, he is a Postdoctoral Research Fellow at the Information and Communication Technologies Center of the Commonwealth Scientific and Industrial Research Organization (CSIRO), Marsfield, Australia. His research interests include estimation, target tracking, and wireless localization.

David Humphrey received a combined degree in electrical engineering and physics from the University of New South Wales in 2000, and a Ph.D. in image processing in 2010. He previously worked at Canon, and is currently employed at the Commonwealth Scientific and Industrial Research Organization (CSIRO). His current research interests include time of arrival estimation, wireless localization, and wireless communications.

Mark Hedley was awarded a B.Sc., a B.E. in electronic engineering and a Ph.D. all from the University of Sydney, Australia. He was then a member of the academic staff at the same university for several years before joining the Commonwealth Scientific and Industrial Research Organization (CSIRO) where he presently leads a team within the ICT Center undertaking research in wireless tracking. His other research interests have included medical image processing, video compression, computer vision, acoustic imaging and communication theory.